

# UC San Diego

## UC San Diego Previously Published Works

### Title

Sex and mental health are related to subcortical brain microstructure.

### Permalink

<https://escholarship.org/uc/item/5xk2697n>

### Journal

Proceedings of the National Academy of Sciences, 121(31)

### Authors

Pecheva, Diliana

Smith, Diana

Casey, B

et al.

### Publication Date

2024-07-30

### DOI

10.1073/pnas.2403212121

Peer reviewed



# Sex and mental health are related to subcortical brain microstructure

Diliana Pecheva<sup>a</sup>, Diana M. Smith<sup>ab</sup> , B. J. Casey<sup>c</sup> , Lianne J. Woodward<sup>d</sup> , Anders M. Dale<sup>a,e,f,g</sup> , Christopher G. Filippi<sup>h</sup> , and Richard Watts<sup>d,1</sup>

Edited by Donald Pfaff, Rockefeller University, New York, NY; received February 18, 2024; accepted June 14, 2024

Some mental health problems such as depression and anxiety are more common in females, while others such as autism and attention deficit/hyperactivity (AD/H) are more common in males. However, the neurobiological origins of these sex differences are poorly understood. Animal studies have shown substantial sex differences in neuronal and glial cell structure, while human brain imaging studies have shown only small differences, which largely reflect overall body and brain size. Advanced diffusion MRI techniques can be used to examine intracellular, extracellular, and free water signal contributions and provide unique insights into microscopic cellular structure. However, the extent to which sex differences exist in these metrics of subcortical gray matter structures implicated in psychiatric disorders is not known. Here, we show large sex-related differences in microstructure in subcortical regions, including the hippocampus, thalamus, and nucleus accumbens in a large sample of young adults. Unlike conventional T1-weighted structural imaging, large sex differences remained after adjustment for age and brain volume. Further, diffusion metrics in the thalamus and amygdala were associated with depression, anxiety, AD/H, and antisocial personality problems. Diffusion MRI may provide mechanistic insights into the origin of sex differences in behavior and mental health over the life course and help to bridge the gap between findings from experimental, epidemiological, and clinical mental health research.

brain | sex differences | diffusion MRI

**Sex Differences and Mental Health.** Sex differences are evident in both the developmental onset, prevalence, and phenotypic presentation of mental health problems across the lifespan (1, 2). For example, females have a higher lifetime prevalence of anxiety (M:F 1:1.7) (3) and mood disorders (M:F 1:1.9) (4) than males, whereas autism (M:F 3.3:1) (5), ADHD (M:F 2.2:1) (6) and antisocial behavior are more common in males (7). However, the origins of these sex-based differences in mental health are poorly understood.

Sex differences have been observed in the pharmacokinetics and pharmacodynamics of antipsychotic drugs (8) with a greater side effects burden in females (9). Identifying possible factors that might explain these sex differences is important to both advance understanding of the etiological and pathogenic mechanisms underlying different mental health conditions but also to inform improved diagnosis and treatment to reduce mental health disparities.

One potential explanation is that these differences may reflect differences in the neural mechanisms that underpin neuropsychiatric and neurological disorders (10). Due to the historical overrepresentation of males in both human and animal research (11), we have yet to fully characterize the role of neuroanatomical sex differences in mental health.

**Sex Differences and Macrostructure—Evidence from Humans.** Sex differences have been detected in the volumes of subcortical brain regions previously implicated in neuropsychiatric disorders (12). For example, functional and volumetric alterations in subcortical gray matter structures have been implicated in mood disorders (13). However, after controlling for brain size, sex difference effect sizes are generally small (14, 15). For example, study of approximately 40,000 participants in the UK Biobank (16) identified small but statistically significant male/female differences in a majority (67%) of the 620 structural imaging-derived phenotypes examined, with a median absolute standardized effect size of 0.17 after allometric adjustment for brain size. These human imaging studies have focused on sex differences in macroscopic morphometry (12) rather than on microscopic differences reported in the animal literature.

**Sex Differences and Microstructure—Evidence from Animal Models.** Animal studies have demonstrated sex differences in brain microstructure suggesting that multiple cellular characteristics likely contribute to neuroanatomical differences observed in

## Significance

We demonstrate the presence of large sex-related differences in the microstructure of subcortical gray matter using advanced noninvasive diffusion MRI in a large cohort of young adults. These sex differences are found in several key brain structures that are important for mental health and are consistent with experimental studies in animals showing cellular differences in these regions. Further, we demonstrate that brain imaging measures in regions with large sex differences are also associated with psychiatric symptoms.

Author affiliations: <sup>a</sup>Center for Multimodal Imaging and Genetics, University of California, San Diego, La Jolla, CA 92093; <sup>b</sup>Medical Scientist Training Program, University of California, San Diego, La Jolla, CA 92093; <sup>c</sup>Department of Neuroscience and Behavior, Barnard College, New York, NY 10027; <sup>d</sup>Faculty of Health, University of Canterbury, Christchurch 8140, New Zealand; <sup>e</sup>Department of Radiology, University of California, San Diego, La Jolla, CA 92093; <sup>f</sup>Department of Neurosciences, University of California, San Diego, La Jolla, CA 92093; <sup>g</sup>Department of Psychiatry, University of California, San Diego, La Jolla, CA 92093; and <sup>h</sup>Department of Radiology, The Hospital for Sick Children and the SickKids Research Institute, Toronto, ON M5G 1E8, Canada

Author contributions: B.J.C., A.M.D., C.G.F., and R.W. designed research; D.P. and R.W. performed research; A.M.D. contributed new reagents/analytic tools; D.P., D.M.S., and R.W. analyzed data; and D.P., D.M.S., B.J.C., L.J.W., C.G.F., and R.W. wrote the paper.

Competing interest statement: A.M.D. is a Founder of and holds equity in CorTechs Labs, Inc., and serves on its Scientific Advisory Board. He is a member of the Scientific Advisory Board of Human Longevity, Inc., and the Mohn Medical Imaging and Visualization Centre in Bergen, Norway. He receives funding through research agreements with General Electric Healthcare. The terms of these arrangements have been reviewed and approved by UCSD in accordance with its conflict of interest policies. The other authors declare no competing interests.

This article is a PNAS Direct Submission.

Copyright © 2024 the Author(s). Published by PNAS. This article is distributed under Creative Commons Attribution-NonCommercial-NoDerivatives License 4.0 (CC BY-NC-ND).

<sup>1</sup>To whom correspondence may be addressed. Email: richard.watts@canterbury.ac.nz.

This article contains supporting information online at <https://www.pnas.org/lookup/suppl/doi:10.1073/pnas.2403212121/-DCSupplemental>.

Published July 23, 2024.

adulthood, including volumetric differences. These differences are evident in neuron or glial cell number (17, 18), dendritic complexity, arborization and spine density (19, 20), microglia phagocytosis (21), microglia (22) and astrocyte (23) morphology, and neurogenesis (24), soma size (25), number of excitatory synapses (19), and degree of myelination (26). However, human *in vivo* studies of sex differences in gray matter microstructure are lacking. Thus, it is unclear whether volumetric differences in humans reflect changes in neuron or glial cell number, or other cellular changes such as dendritic density.

### Diffusion MRI—Noninvasive Measure of Microstructure.

Diffusion-weighted MRI (dMRI) provides unique information about the tissue microstructure and organization of the brain *in vivo* (27). Water molecules undergo diffusion due to their thermal energy. In a free medium, molecules traverse a random walk, and their displacement pattern can be characterized by a three-dimensional Gaussian distribution. However, in biological tissues, the microstructural environment hinders or restricts the diffusion of water molecules. By measuring their displacement pattern in the brain, it is possible to distinguish between different tissue environments. The diffusion of water molecules in the extracellular space is hindered by the presence of cell soma and processes, while water molecules in the intracellular space are restricted by cell membranes. The orientation of cellular microstructures influences the direction in which water molecules diffuse, resulting in isotropic or anisotropic diffusion. The signal measured by dMRI is sensitive to properties such as cell size, cell density, myelination, and axonal and dendritic structure. Therefore, dMRI has the potential to identify sex differences in humans beyond brain structure volumes, reflecting a range of these neurobiological processes.

To date, dMRI has most often been used to assess white matter integrity and possible white matter sex differences (28). However, multicompartiment models of diffusion such as neurite orientation dispersion and density imaging (29) and restriction spectrum imaging (RSI) (30) can also provide important metrics relating to gray matter microstructure. The RSI model provides measures of the intracellular, extracellular, and free water (cerebrospinal fluid) environments making it an ideal candidate with which to assess gray matter microstructure. It has been successfully applied to study subcortical and cortical gray matter, and white matter in adult and developmental populations (28, 31, 32). RSI may therefore be a useful method for examining sex differences in subcortical gray matter with greater tissue specificity *in vivo* in the human brain.

**Overview.** In this paper, we investigate sex-related differences in the microstructure of subcortical gray matter regions in a large cohort of young adults assessed using noninvasive dMRI. We hypothesize that any observed sex-related differences in regional gray matter microstructure would also be associated with mental health problems known to vary by sex, including the extent of depression, anxiety, attention deficit/hyperactivity (AD/H), and antisocial behavior symptomatology.

## Results

**Study Population.** The sample consisted of 1,065 ( $n = 575$  female,  $n = 490$  male) participants from 436 families who were enrolled in the Human Connectome Project (HCP) Young Adult study (33). The characteristics of the sample are shown in Table 1. Females were significantly older ( $29.5 \pm 3.6$  vs.  $27.9 \pm 3.6$  y,  $P < 0.001$ ), had somewhat lower body mass index (BMI) ( $26.1 \pm 5.7$  vs.  $26.8 \pm 4.3$  kg/m<sup>2</sup>,  $P = 0.034$ ), and significantly lower supratentorial

volume ( $0.968 \pm 0.082$  vs.  $1.111 \pm 0.093$  L,  $P < 0.001$ ). The subpopulation of unrelated subjects had similar characteristics.

**Main Effect of Sex.** Fig. 1 shows voxelwise analysis by sex for unrelated subjects. Males had strongly decreased hindered isotropic signal in the thalamus, caudate, nucleus accumbens, and brainstem and increased restricted isotropic signal in the amygdala/hippocampus than females. *SI Appendix, Figs. S2 and S3* show mean hindered and restricted isotropic component maps for the unrelated male and female participants corresponding to Fig. 1. *SI Appendix, Figs. S4–S23* show whole-brain data for the restricted and hindered isotropic components, mean diffusivity, and fractional anisotropy for analyses with and without supratentorial volume and voxelwise Jacobian determinant included in the model. The group level statistical maps are available to download from the Brain Analysis Library of Spatial maps and Atlases database, <https://balsa.wustl.edu/study/r330M>.

Controlling for age, BMI, supratentorial, and regional volume using a mixed effect model (Table 2), significant ( $P < 0.05$  after Bonferroni correction for multiple comparisons) effects of sex on diffusion were found in 27/32 regions/metrics. In each of the hippocampus, amygdala, thalamus, caudate, nucleus accumbens, and brainstem, one or more diffusion metrics were highly significant with  $P < 10^{-16}$ . The largest standardized effect sizes for the hindered isotropic component were in the hippocampus ( $-0.92 \pm 0.06$ ) and thalamus ( $-0.87 \pm 0.06$ ), where negative values represent a lower signal in males compared to females. The hippocampus also demonstrated the largest effect sizes in the restricted isotropic component ( $0.75 \pm 0.06$ ), representing a larger signal in males compared to females and the restricted directional component ( $-0.78 \pm 0.07$ ) compared to other regions studied. The largest standardized effect size for volume was the amygdala at  $0.54 \pm 0.07$ .

*SI Appendix, Table S1* shows the corresponding Cohen's  $d$  values. Without accounting for other covariates, the maximum absolute value was  $d = -1.63$  (95% CI 1.41, 1.85) for the hindered isotropic component in the thalamus. For comparison, supratentorial volume was larger in males, with  $d = 1.65$  (95% CI 1.43 to 1.87). As shown in Fig. 2, the degree of overlap in the thalamus hindered isotropic diffusion component between males and females was similar to the overlap in supratentorial volume, as would be expected from their comparable effect sizes.

For the most significant region and metric, the hindered isotropic component in the thalamus, sex alone explained 39.8% of the variance in the metric. Including the remaining covariates in the analysis showed that the unique variance explained by sex was 11.4% (eta-squared).

Data from 45 participants who had repeated imaging showed good test–retest reliability in the imaging metrics. For example, an intraclass correlation of 0.893 was obtained for the hindered isotropic component in the thalamus (Fig. 3).

**Emotional and Behavioral Adjustment Problems.** Females displayed greater anxiety ( $P < 0.001$ ) and somatotopic ( $P = 0.001$ ) problems, while males scored higher on measures of avoidance ( $P = 0.003$ ), AD/H ( $P < 0.001$ ), and antisocial behavior problems ( $P < 0.001$ ; see Table 1).

Full statistics for the association of Achenbach-based, Diagnostic and Statistical Manual of Mental Disorders (DSM) raw scores with all diffusion metrics are available in *SI Appendix, Tables S3–S8*. The regions and metrics that were significant after Bonferroni correction ( $P < 0.05$ ,  $n_{\text{Tests}} = 192$ ,  $P_{\text{Uncorrected}} < 2.6 \times 10^{-4}$ ) are shown in Table 3. The amygdala demonstrated significant associations with depression and antisocial personality; the thalamus with depression, anxiety, AD/H, and antisocial personality.

**Table 1. Characteristics of study participants by self-reported sex for the total sample (n = 1,065), and the subsample of unrelated subjects (n = 436)**

	Full sample			Unrelated		
	Females	Males	<i>P</i>	Females	Males	<i>P</i>
N	575 (54.0%)	490 (46.0%)		234 (53.7%)	202 (46.3%)	
Age (years)	29.5 (3.6)	27.9 (3.6)	<0.001	29.4 (3.6)	27.6 (3.6)	<0.001
BMI (kg/m <sup>2</sup> )	26.1 (5.7)	26.8 (4.3)	0.034	26.5 (6.1)	26.9 (4.4)	0.462
Supratentorial volume (liters)	0.968 (0.082)	1.111 (0.093)	<0.001	0.966 (0.083)	1.111 (0.093)	<0.001
Race			0.317			0.658
White	420 (73.0%)	383 (78.2%)		163 (69.7%)	153 (75.7%)	
Black	94 (16.3%)	56 (11.4%)		38 (16.2%)	24 (11.9%)	
Asian/Pacific Is.	35 (6.1%)	30 (6.1%)		17 (7.3%)	15 (7.4%)	
Other/Unknown	26 (4.5%)	21 (4.3%)		16 (6.8%)	10 (5.0%)	
Hispanic Ethnicity	42 (7.3%)	52 (10.6%)	0.135	24 (10.3%)	22 (10.9%)	0.497
Zygosity			0.703			0.304
Dizygotic twin	97	63		34	18	
Monozygotic twin	162	116		61	49	
Mental Health						
Depression	3 (2, 6)	3 (2, 6)	0.274	4 (2, 7)	3 (2, 6)	0.012
Anxiety	4 (2, 6)	3 (2, 5)	<0.001	4 (3, 6)	3 (2, 5)	<0.001
Somatic	1 (0, 2)	1 (0, 2)	0.001	1 (0, 3)	0.5 (0, 2)	0.057
Avoidance	2 (1, 4)	3 (1, 4)	0.003	2 (1, 4)	3 (1, 4.75)	0.199
AD/H	5 (2, 7)	6 (3, 9)	<0.001	5 (2, 8)	5 (3, 9)	0.328
Antisocial	2 (1, 4)	3 (1, 5)	<0.001	2 (1, 4)	3 (2, 6)	<0.001

Continuous variables listed as mean (SD), *P*-values calculated using a Welch two sample *t* test. Mental health raw scores listed as median (interquartile range); *P*-values calculated using a Wilcoxon rank sum test.

## Discussion

**Common Features and Comparison to Human Literature.** Across the subcortical gray matter regions considered, in general, males displayed higher restricted isotropic diffusion and lower restricted directional diffusion (Table 2). Consistent with this result, using a conventional diffusion tensor model, males had lower fractional anisotropy than females (*SI Appendix, Table S2*). Anisotropy may reflect changes in dendritic structure, consistent with changes in axonal myelination or dendritic complexity, arborization, and spine density (19, 20).

The shift in signal from the higher-diffusivity hindered component to the lower-diffusivity restricted component in males compared to females is also reflected in decreased mean diffusivity. This finding suggests greater intracellular signal in males, which could be due to increased cellularity, gliosis, or changes in cell morphology.

The associations between diffusion metrics and the extent of mental health problems were weaker but showed consistent trends. Increased restricted isotropic and decreased hindered isotropic signal in the amygdala and thalamus, respectively, were associated with greater mental health problems. In general, more male-like diffusion metrics (increased restricted isotropic, decreased hindered isotropic and restricted directional signal) were associated with poorer mental health functioning, including anxiety and depression symptoms that are more prevalent in females than males. This finding is consistent with increased male genetic vulnerability (34).

**Previously Reported Effect Sizes.** In the largest study of neuroanatomical norms for sex and age (n = 40,028, ages 40 to 69) (16), statistically significant sex differences after allometric adjustment for total brain volume were found in 67% of measures, although the median absolute effect size was modest (0.13). Subcortical

volume differences were similarly small, with effect sizes ranging from 0.06 (left hippocampus) to 0.18 (putamen). This study challenged the view that “once we account for individual differences in brain size, there is almost no difference in the volume of specific cortical or subcortical structures between men and women” (14).

It is surprising that the large effect sizes reported here have not been described previously. However, diffusion MRI is much more commonly applied to white matter than to subcortical gray matter structures. The use of a more advanced analysis technique (RSI) compared to a conventional diffusion tensor model may have increased our sensitivity to sex-related differences, although we found consistent results using both diffusion tensor imaging and RSI (*SI Appendix, Table S2*). This suggests that our results may benefit from but are not unique to the specific model selected. Our participant population were sexually mature young adults, and therefore, any differential effects of puberty on development are likely to be irrelevant. Previous studies have often concentrated on either developmental or older cohorts.

**Androgen Receptors in the Brain.** We found increased restricted isotropic signal in males compared to females in several regions, including multiple subcortical structures known to contain high densities of androgen receptors, including the thalamus, hippocampus, and amygdala (35). In animal models, brain structures that are sensitive to androgen administration are larger in males than in females (36), and testosterone has been shown to influence amygdala morphology in rodent studies (37). For example, pubertal testosterone increases neurogenesis in the medial amygdala of male rats (17), and circulating androgens are known to play an important role in the maintenance of the greater posterodorsal subnucleus of the medial amygdala (17, 38). Based on this literature,

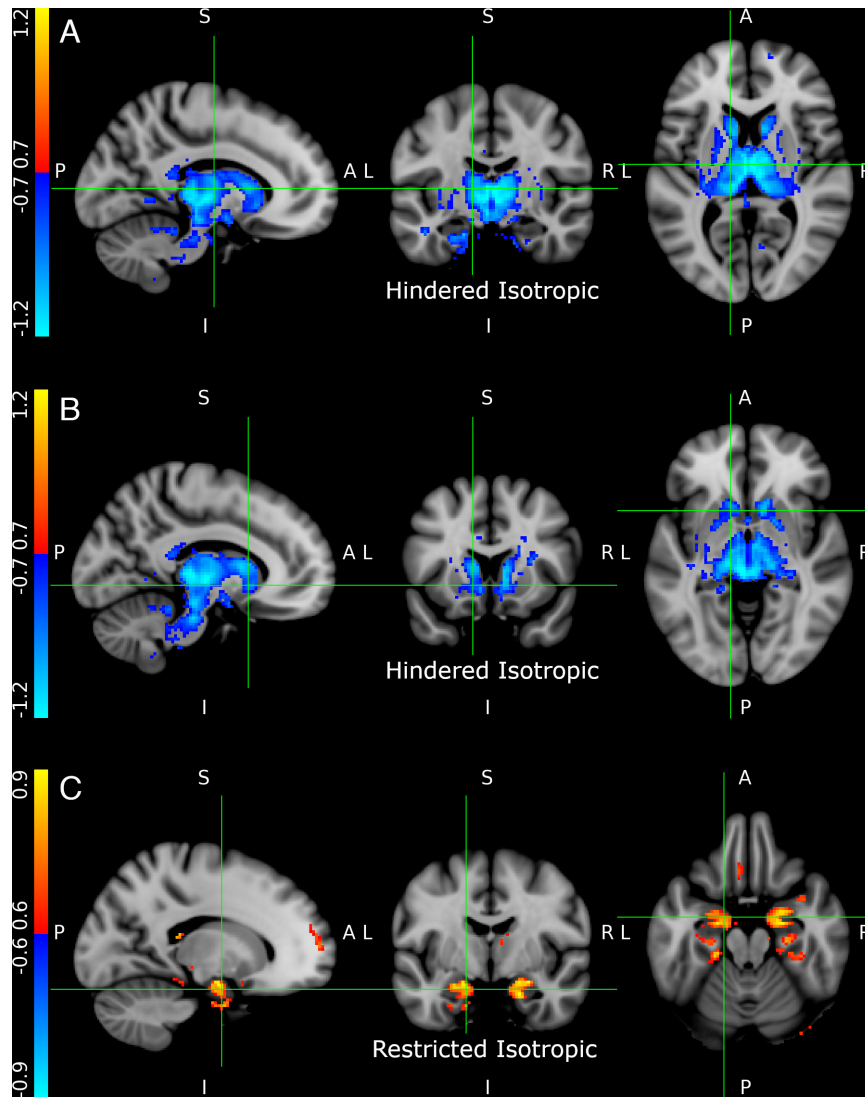


**Fig. 1.** Voxelwise analysis of differences in hindered and restricted isotropic signal with sex after accounting for age and BMI. Decreased hindered isotropic signal is observed in the thalamus, caudate, nucleus accumbens, and brainstem of males (A and B). Increased restricted isotropic signal is observed in the amygdala and hippocampus in males (C). Color scale represents standardized effect sizes, with red-yellow indicating males greater than females and blue-cyan males less than females. Corresponding sections on the T1-weighted underlay images and diffusion parameter maps separately for males and females are shown in *SI Appendix, Figs. S1–S3*. Sagittal, coronal, and axial sections are shown corresponding to MNI coordinates (−12, −12, 7) (A), (−11, 13, −4) (B), and (−16, −6, −21) (C).

it is possible that testosterone acts directly on astrocytes to influence their structure and function.

Developmental trajectories of certain brain regions have been found to align with pubertal changes more closely than with age in humans, suggesting an androgenic basis for sex differences in

brain morphology (39). In a study of 433 children and adolescents aged 4 to 24 y (40), DHEA and testosterone were both associated with cortical thickness as well as multiple cortical–subcortical networks, which may indicate hormonal effects on structural connectivity between the cortex and subcortical structures such as the

**Table 2. Standardized effect size (beta ± SE) of sex on diffusion metrics and regional volume from a mixed effects model that includes age, BMI, and supratentorial volume as covariates**

Region	Restricted isotropic	Hindered isotropic	Free water	Restricted directional	Volume
Hippocampus	0.75 ± 0.06*	−0.92 ± 0.06*	0.63 ± 0.07*	−0.78 ± 0.07*	0.22 ± 0.07*
Amygdala	0.66 ± 0.06*	−0.54 ± 0.07*	0.15 ± 0.08	−0.65 ± 0.08*	0.54 ± 0.07*
Thalamus	0.28 ± 0.08*	−0.87 ± 0.06*	0.70 ± 0.07*	−0.75 ± 0.07*	0.30 ± 0.04*
Caudate	0.50 ± 0.07*	−0.67 ± 0.06*	0.37 ± 0.07*	0.04 ± 0.08	−0.01 ± 0.06
Pallidum	0.14 ± 0.08	−0.42 ± 0.07*	0.33 ± 0.08*	−0.44 ± 0.08*	0.36 ± 0.06*
Putamen	0.13 ± 0.07	−0.34 ± 0.07*	0.40 ± 0.07*	−0.28 ± 0.08*	0.32 ± 0.05*
Nucleus Accumbens	0.48 ± 0.08*	−0.84 ± 0.07*	0.56 ± 0.07*	−0.13 ± 0.08	0.02 ± 0.07
Brainstem	0.46 ± 0.07*	−0.78 ± 0.06*	0.53 ± 0.07*	−0.48 ± 0.08*	0.22 ± 0.07

Regional volume was also included as a covariate for diffusion metrics. Positive values indicate that the metric is higher in males than females. \* Indicates Bonferroni corrected  $P < 0.05$  with  $n_{\text{Tests}} = 40$  ( $P_{\text{Uncorrected}} < 0.00125$ ).

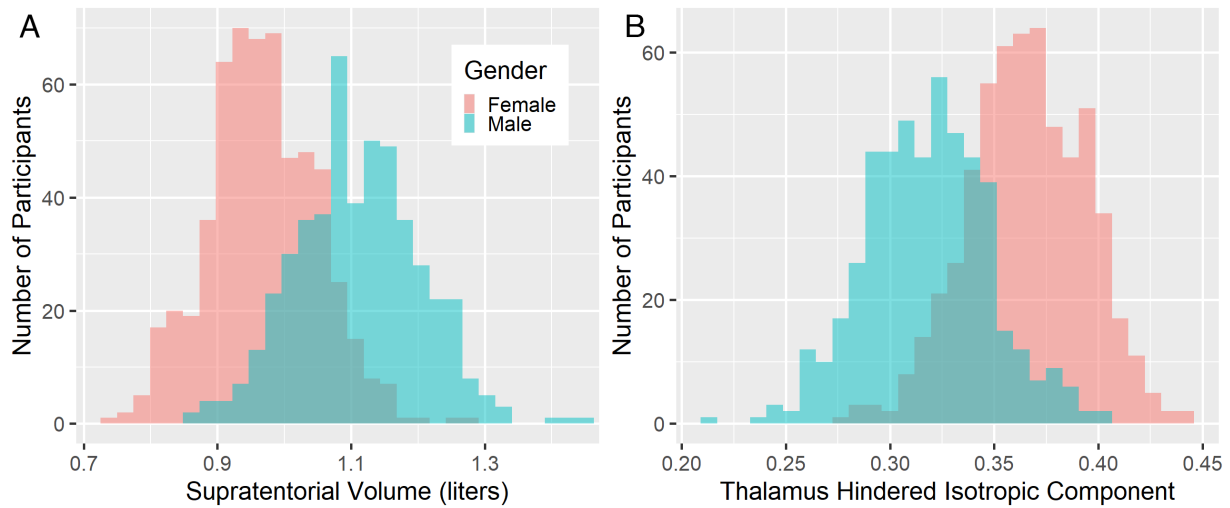


**Fig. 2.** Distributions of (A) supratentorial volume (Cohen's  $d = 1.65$ ) and (B) the hindered component of diffusion in the thalamus (Cohen's  $d = 1.63$ ).

amygdala and hippocampus (40). Of note, although we did not examine the hypothalamus as a specific region of interest in this work, the preoptic nucleus of the hypothalamus is known to differ phenotypically between males and females (41); examining the microstructure of the hypothalamus through diffusion MRI in humans may be a promising avenue for future research.

**Associations with Mental Health Functioning.** Greater restricted isotropic signal in the amygdala was associated with depression and antisocial personality. Acute and chronic stress can precipitate the development of depression (42), and stress has been shown to result in long-lasting dendritic hypertrophy in the amygdala (43–45). Dendritic hypertrophy would increase the intracellular compartment resulting in an increase in the restricted isotropic component of the diffusion signal.

Lower hindered isotropic signal and greater free water signal in the thalamus were associated with greater DSM raw scores for depression, anxiety, AD/H and antisocial personality. Thalamocortical circuits are essential for motor, sensory, and cognitive processing (46), and impairment in these functions is known to be implicated in psychiatric disorders (47).

Animal studies have also shown that extracellular matrix alterations occur in cortical and subcortical gray matter with stress and

have been related to depressive phenotypes (48). Changes in the extracellular environment would be reflected in the hindered diffusion compartment. Exactly how this relates to reduced hindered isotropic signal in the thalamus is yet unclear. Disruptions to the extracellular matrix have also been shown in schizophrenia and bipolar disorder patients and have been inferred to contribute to disruptions in sleep patterns, emotional and cognitive processing, and attention (49). Although we did not assess measures related to these disorders, difficulties in these everyday functions are characteristic of the mental health problems examined in our analysis.

The thalamus has been implicated in regulating anxiety-related responses by modulating neuronal output via its interface with prefrontal cortex pathways and the amygdala (46). Functional impairment of the thalamic reticular nucleus (TRN) has been shown to induce attention deficits, hyperactivity, and sleep disruption (50) and projections from the amygdala to the TRN have been posited to play a part in controlling emotional attention via the suppression of irrelevant stimuli (51). In addition, the pulvinar nucleus of the thalamus is generally understood to be involved in visual processing and distractor filtering, with structural and functional imaging studies finding associations between the pulvinar nucleus and AD/H in human samples (52).

**Limitations and Future Work.** Participants in the Human Connectome Project (HCP) study were asked their gender rather than their biological sex, which are not equivalent. Sex, typically assigned at birth, refers to anatomical and physiological traits such as chromosomes, external genitalia, and secondary sex characteristics. Gender refers to socially constructed roles and behaviors that link gender identity and expression in a cultural context. Trying to parse the unique and shared variance in brain microstructure explained by sex and gender is not possible using this dataset. Furthermore, this study only permitted a binary choice of “male” or “female” gender, without consideration for other gender identities.

The HCP dataset is not enriched for participants with mental health problems, limiting our statistical power to detect interactions between sex and gender. Given the dataset available, we can only hypothesize that differences in subcortical microstructure provide a neuroanatomical substrate for sex differences in mental health phenotypes. Future analyses should directly assess these associations using datasets sufficiently powered to do so.

Sex differences are not constant throughout the lifespan; therefore we should study populations of different ages. The Adolescent Brain Cognitive Development study (ABCD Study<sup>®</sup>) (53) follows more

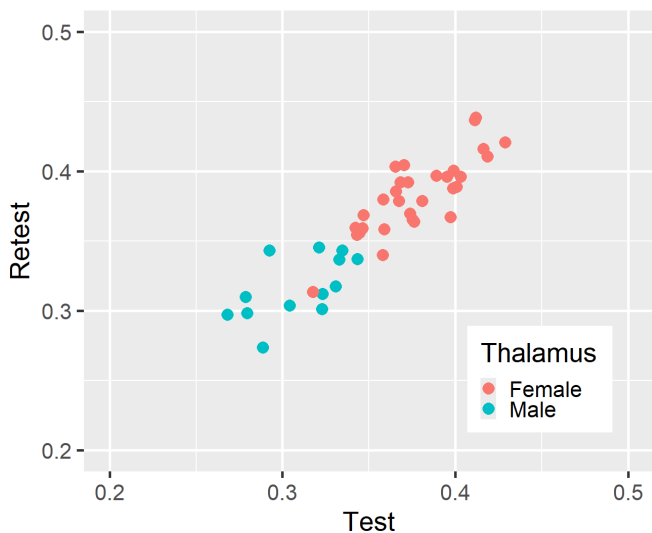


**Fig. 3.** Test–retest comparison for the hindered isotropic component of diffusion in the thalamus. The intraclass correlation is 0.893.

**Table 3. Regions and metrics significantly associated with DSM raw scores ( $P < 0.05$ ,  $n_{\text{Tests}} = 192$ ,  $P_{\text{Uncorrected}} < 2.6 \times 10^{-4}$ )**

DSM	Region	Metric	t	P
Depression	Amygdala	Restricted isotropic	3.76	$1.8 \times 10^{-4}$
	Thalamus	Hindered isotropic	-4.81	$1.7 \times 10^{-6}$
		Free	4.15	$3.6 \times 10^{-5}$
Anxiety	Thalamus	Hindered isotropic	-4.00	$6.8 \times 10^{-5}$
AD/H	Thalamus	Hindered isotropic	-4.13	$3.9 \times 10^{-5}$
	Thalamus	Free	3.91	$1.0 \times 10^{-4}$
Antisocial personality	Amygdala	Restricted isotropic	4.26	$2.3 \times 10^{-5}$
	Thalamus	Hindered isotropic	-3.74	$1.9 \times 10^{-4}$

Uncorrected  $P$ -values are shown.

than 10,000 children from age 9 to 10 to young adulthood with imaging every 2 y for 10 y. It is expected that the differences reported here in young adults will emerge before the conclusion of ABCD. The UK Biobank enrolled a very large population of participants aged 40 to 69, and we would hypothesize that sex-related differences in brain structure may decrease with age and hormone levels in this population.

## Conclusions

We have demonstrated large effects (standardized effect size over 0.9 while including age, BMI, and supratentorial volume as covariates) of sex on subcortical gray matter microstructure in many regions, particularly the amygdala, hippocampus, caudate, and thalamus, in a large population of young adults. These effect sizes are substantially greater than any sex-brain imaging associations observed previously, apart from simple brain size, with sex differences explaining 40% of the variance in a microstructure metric in the thalamus. The microstructure of the thalamus and amygdala were also significantly associated with depression, anxiety, AD/H, and antisocial personality problems. This study may shed light on the mechanisms underlying these behavioral differences, and sex differences in the susceptibility of males and females to different mental health problems.

## Materials and Methods

**HCP Data.** Data were obtained from the HCP1200 release of the Human Connectome Project Young Adult study (33, 54). 1,065 participants from 436 families had complete preprocessed diffusion data ( $n = 575$  female,  $n = 490$  male). Sex was defined based on self-reported gender rather than biological sex, using the binary choice of male or female. While we refer to sex throughout this paper, we use gender as a proxy for sex.

The imaging protocol (55) included almost an hour of diffusion data acquisition on a customized Siemens 3T MRI scanner, including high angular resolution data acquired at  $b$ -values of 1,000, 2,000, and 3,000  $\text{s/mm}^2$ , with an isotropic spatial resolution of 1.25 mm and full brain coverage.

Data were preprocessed according to Glasser et al. (56). Diffusion preprocessing included correction for subject motion, susceptibility, and eddy-current distortions (57, 58). Subcortical regions were defined using FMRIB Image Registration and Segmentation Tool (FIRST) (59), while supratentorial volumes were derived using FreeSurfer (60). Prior to fitting the RSI model, diffusion data were smoothed using a gaussian filter with  $\sigma = 1.0$  mm. For the voxelwise analysis, data were transformed into MNI152 atlas space using FMRIB Nonlinear Image Registration Tool (FNIRT).

Measures of the extent of depression, anxiety, somatic, avoidant personality, AD/H, and antisocial personality problems were obtained using the Achenbach Adult Self-Report scale (61). Raw subscale scores for each outcome measure are reported.

**RSI.** The RSI model (30) was implemented using Python. Diffusion was modeled using three compartments: a restricted compartment with  $D_{\text{Longitudinal}} = 1.0 \times 10^{-3} \text{ mm}^2/\text{s}$ ,  $D_{\text{Transverse}} = 0 \text{ mm}^2/\text{s}$ ; a hindered compartment with  $D_{\text{Longitudinal}} = 1.0 \times 10^{-3} \text{ mm}^2/\text{s}$ ,  $D_{\text{Transverse}} = 0.9 \times 10^{-3} \text{ mm}^2/\text{s}$ ; and a free compartment with  $D_{\text{Longitudinal}} = D_{\text{Transverse}} = 3.0 \times 10^{-3} \text{ mm}^2/\text{s}$  (62). Diffusion-weighted signals were normalized to give unit signal for  $b = 0 \text{ s/mm}^2$ . The primary imaging outcome variables were the isotropic components for the three compartments and the directional component of the restricted compartment.

**Statistical Models.** Statistical significance was determined using two-sided  $t$  tests with  $P < 0.05$  and Bonferroni correction for multiple comparison.

Voxelwise analysis was performed using the general linear model implemented in Permutation Analysis of Linear Models (PALM) (63). For the voxelwise analysis, only a single participant from each of the 436 families was used, with age, sex, and BMI as explanatory variables. RSI metrics have previously been shown to be strongly associated with both age and BMI in adolescents (31, 32).

Region-wise analysis used the linear mixed effects model (lmerTest) implemented in R 4.3.0, using all subjects, with family ID included as a random effect. To determine whether sex differences in diffusion metrics were driven by global or regional brain volume rather than as a direct result of sex, these variables were included in the lmer model:

$$\text{RSImetric\_region} \sim \text{Age} + \text{Gender} + \text{BMI} + \text{STvolume} + \text{vol\_region} + (1 | \text{Family\_ID}),$$

where STvolume represents the supratentorial volume. To determine standardized effect sizes, continuous variables were normalized to a mean of zero and a SD of unity, apart from age, which was only normalized to the mean. Sex was coded as zero for females and one for males. Effect sizes were also calculated after residualizing for supratentorial volume. Cohen's  $d$  values were calculated using the lsr package in R (version 4.3.0).

Achenbach Adult Self-Report DSM raw scores for depression, anxiety, somatic, avoidant personality, AD/H, and antisocial personality problems were analyzed using a similar mixed effects model, with age and sex as additional covariates:

$$\text{DSM\_raw} \sim \text{Age} + \text{Gender} + \text{RSImetric\_region} + (1 | \text{Family\_ID}).$$

$P$ -values were Bonferroni corrected at  $P < 0.05$  for 4 metrics  $\times$  8 regions  $\times$  6 DSM scores,  $P_{\text{Uncorrected}} < 2.6 \times 10^{-4}$ .

**Data, Materials, and Software Availability.** Source data were obtained from the Human Connectome Project 1200 Subjects Data Release, Diffusion Preprocessed package <https://www.humanconnectome.org/study/hcp-young-adult> (54). The RSI model fitting code is available at <https://github.com/ABCD-STUDY> (64).

**ACKNOWLEDGMENTS.** Data were provided in part by the Human Connectome Project, WU-Minn Consortium (Principal Investigators: David Van Essen and Kamil Ugurbil; 1U54MH091657) funded by the 16 NIH Institutes and Centers that support the NIH Blueprint for Neuroscience Research and by the McDonnell Center for Systems Neuroscience at Washington University.

1. S. Dalsgaard *et al.*, Incidence rates and cumulative incidences of the full spectrum of diagnosed mental disorders in childhood and adolescence. *JAMA Psychiatry* **77**, 155–164 (2020).
2. C. B. Pedersen *et al.*, A comprehensive nationwide study of the incidence rate and lifetime risk for treated mental disorders. *JAMA Psychiatry* **71**, 573–581 (2014).
3. C. P. McLean, A. Asnaani, B. T. Litz, S. G. Hofmann, Gender differences in anxiety disorders: Prevalence, course of illness, comorbidity and burden of illness. *J. Psychiatr. Res.* **45**, 1027–1035 (2011).
4. R. H. Salk, J. S. Hyde, L. Y. Abramson, Gender differences in depression in representative national samples: Meta-analyses of diagnoses and symptoms. *Psychol. Bull.* **143**, 783–822 (2017).
5. R. Loomes, L. Hull, W. P. L. Mandy, What is the male-to-female ratio in autism spectrum disorder? A systematic review and meta-analysis. *J. Am. Acad. Child Adolesc. Psychiatry* **56**, 466–474 (2017).
6. G. Polanczyk, M. S. de Lima, B. L. Horta, J. Biederman, L. A. Rohde, The worldwide prevalence of ADHD: A systematic review and meta-regression analysis. *Am. J. Psychiatry* **164**, 942–948 (2007).
7. P. Pinares-García, M. Stratikopoulos, A. Zagato, H. Loke, J. Lee, Sex: A significant risk factor for neurodevelopmental and neurodegenerative disorders. *Brain Sci.* **8**, 154 (2018).
8. B. A. Brand *et al.*, Antipsychotic medication for women with schizophrenia spectrum disorders. *Psychol. Med.* **52**, 649–663 (2022).
9. T. S. J. Iversen *et al.*, Side effect burden of antipsychotic drugs in real life - Impact of gender and polypharmacy. *Prog. Neuropsychopharmacol. Biol. Psychiatry* **82**, 263–271 (2018).
10. S. Bolte *et al.*, Sex and gender in neurodevelopmental conditions. *Nat. Rev. Neurol.* **19**, 136–159 (2023).
11. S. E. Geller *et al.*, The more things change, the more they stay the same: A study to evaluate compliance with inclusion and assessment of women and minorities in randomized controlled trials. *Acad. Med.* **93**, 630–635 (2018).
12. A. N. Ruigrok *et al.*, A meta-analysis of sex differences in human brain structure. *Neurosci. Biobehav. Rev.* **39**, 34–50 (2014).
13. S. J. Russo, E. J. Nestler, The brain reward circuitry in mood disorders. *Nat. Rev. Neurosci.* **14**, 609–625 (2013).
14. L. Eliot, A. Ahmed, H. Khan, J. Patel, Dump the "dimorphism": Comprehensive synthesis of human brain studies reveals few male-female differences beyond size. *Neurosci. Biobehav. Rev.* **125**, 667–697 (2021).
15. C. Sanchis-Segura *et al.*, Sex differences in gray matter volume: How many and how large are they really? *Biol. Sex Differ.* **10**, 32 (2019).
16. C. M. Williams, H. Peyre, R. Toro, F. Ramus, Neuroanatomical norms in the UK Biobank: The impact of allometric scaling, sex, and age. *Hum. Brain Mapp.* **42**, 4623–4642 (2021).
17. E. I. Ahmed *et al.*, Pubertal hormones modulate the addition of new cells to sexually dimorphic brain regions. *Nat. Neurosci.* **11**, 995–997 (2008).
18. W. A. Koss, M. M. Lloyd, R. N. Sadowski, L. M. Wise, J. M. Juraska, Gonadectomy before puberty increases the number of neurons and glia in the medial prefrontal cortex of female, but not male, rats. *Dev. Psychobiol.* **57**, 305–312 (2015).
19. B. M. Cooke, C. S. Woolley, Effects of prepubertal gonadectomy on a male-typical behavior and excitatory synaptic transmission in the amygdala. *Dev. Neurobiol.* **69**, 141–152 (2009).
20. W. A. Koss, C. E. Belden, A. D. Hristov, J. M. Juraska, Dendritic remodeling in the adolescent medial prefrontal cortex and the basolateral amygdala of male and female rats. *Synapse* **68**, 61–72 (2014).
21. J. W. VanRyzin *et al.*, Microglial phagocytosis of newborn cells is induced by endocannabinoids and sculpt sex differences in juvenile rat social play. *Neuron* **102**, 435–449.e6 (2019).
22. K. M. Lenz, B. M. Nugent, R. Haliyur, M. M. McCarthy, Microglia are essential to masculinization of brain and behavior. *J. Neurosci.* **33**, 2761–2772 (2013).
23. J. A. Mong, M. M. McCarthy, Ontogeny of sexually dimorphic astrocytes in the neonatal rat arcuate. *Brain Res. Dev. Brain Res.* **139**, 151–158 (2002).
24. J. M. Bowers, J. Waddell, M. M. McCarthy, A developmental sex difference in hippocampal neurogenesis is mediated by endogenous oestradiol. *Biol. Sex Differ.* **1**, 8 (2010).
25. R. D. Romeo, C. L. Sisk, Pubertal and seasonal plasticity in the amygdala. *Brain Res.* **889**, 71–77 (2001).
26. J. M. Juraska, J. A. Markham, The cellular basis for volume changes in the rat cortex during puberty: White and gray matter. *Ann. N. Y. Acad. Sci.* **1021**, 431–435 (2004).
27. D. Le Bihan *et al.*, MR imaging of intravoxel incoherent motions: Application to diffusion and perfusion in neurologic disorders. *Radiology* **161**, 401–407 (1986).
28. K. E. Lawrence *et al.*, White matter microstructure shows sex differences in late childhood: Evidence from 6797 children. *Hum. Brain Mapp.* **44**, 535–548 (2023).
29. H. Zhang, T. Schneider, C. A. Wheeler-Kingshott, D. C. Alexander, NODDI: Practical in vivo neurite orientation dispersion and density imaging of the human brain. *Neuroimage* **61**, 1000–1016 (2012).
30. N. S. White, T. B. Leergaard, H. D'Arceuil, J. G. Bjaalie, A. M. Dale, Probing tissue microstructure with restriction spectrum imaging: Histological and theoretical validation. *Hum. Brain Mapp.* **34**, 327–346 (2013).
31. C. E. Palmer *et al.*, Microstructural development from 9 to 14 years: Evidence from the ABCD Study. *Dev. Cogn. Neurosci.* **53**, 101044 (2022).
32. K. M. Rapuano *et al.*, Nucleus accumbens cytoarchitecture predicts weight gain in children. *Proc. Natl. Acad. Sci. U.S.A.* **117**, 26977–26984 (2020).
33. D. C. Van Essen *et al.*, The WU-Minn human connectome project: An overview. *Neuroimage* **80**, 62–79 (2013).
34. P. N. Pallier *et al.*, Chromosomal and environmental contributions to sex differences in the vulnerability to neurological and neuropsychiatric disorders: Implications for therapeutic interventions. *Prog. Neurobiol.* **219**, 102353 (2022).
35. L. L. DonCarlos *et al.*, Novel cellular phenotypes and subcellular sites for androgen action in the forebrain. *Neuroscience* **138**, 801–807 (2006).
36. B. Filova, D. Ostatnikova, P. Celec, J. Hodosy, The effect of testosterone on the formation of brain structures. *Cells Tissues Organs* **197**, 169–177 (2013).
37. D. Marwha, M. Halari, L. Eliot, Meta-analysis reveals a lack of sexual dimorphism in human amygdala volume. *Neuroimage* **147**, 282–294 (2017).
38. B. M. Cooke, G. Tabibnia, S. M. Breedlove, A brain sexual dimorphism controlled by adult circulating androgens. *Proc. Natl. Acad. Sci. U.S.A.* **96**, 7538–7540 (1999).
39. S. Neufang *et al.*, Sex differences and the impact of steroid hormones on the developing human brain. *Cereb. Cortex* **19**, 464–473 (2009).
40. T. V. Nguyen, Developmental effects of androgens in the human brain. *J. Neuroendocrinol.* **30**, e12486 (2018).
41. M. A. Hofman, D. F. Swaab, The sexually dimorphic nucleus of the preoptic area in the human brain: A comparative morphometric study. *J. Anat.* **164**, 55–72 (1989).
42. T. L. Bale, Stress sensitivity and the development of affective disorders. *Horm. Behav.* **50**, 529–533 (2006).
43. M. N. Hill, C. J. Hillard, B. S. McEwen, Alterations in corticolimbic dendritic morphology and emotional behavior in cannabinoid CB1 receptor-deficient mice parallel the effects of chronic stress. *Cereb. Cortex* **21**, 2056–2064 (2011).
44. R. Mitra, S. Jadhav, B. S. McEwen, A. Vyas, S. Chattarji, Stress duration modulates the spatiotemporal patterns of spine formation in the basolateral amygdala. *Proc. Natl. Acad. Sci. U.S.A.* **102**, 9371–9376 (2005).
45. A. Vyas, S. Jadhav, S. Chattarji, Prolonged behavioral stress enhances synaptic connectivity in the basolateral amygdala. *Neuroscience* **143**, 387–393 (2006).
46. M. M. Kenwood, N. H. Kalin, H. Barbas, The prefrontal cortex, pathological anxiety, and anxiety disorders. *Neuropsychopharmacology* **47**, 260–275 (2022).
47. S. Parnaudeau, S. S. Bolkan, C. Kellendonk, The mediodorsal thalamus: An essential partner of the prefrontal cortex for cognition. *Biol. Psychiatry* **83**, 648–656 (2018).
48. I. Blanco, K. Conant, Extracellular matrix remodeling with stress and depression: Studies in human, rodent and zebrafish models. *Eur. J. Neurosci.* **53**, 3879–3888 (2021).
49. P. Steullet *et al.*, The thalamic reticular nucleus in schizophrenia and bipolar disorder: Role of parvalbumin-expressing neuron networks and oxidative stress. *Mol. Psychiatry* **23**, 2057–2065 (2018).
50. M. F. Wells, R. D. Wimmer, L. I. Schmitt, G. Feng, M. M. Halassa, Thalamic reticular impairment underlies attention deficit in Ptchd1(Y<sup>-</sup>) mice. *Nature* **532**, 58–63 (2016).
51. B. Zikopoulos, H. Barbas, Pathways for emotions and attention converge on the thalamic reticular nucleus in primates. *J. Neurosci.* **32**, 5338–5350 (2012).
52. J. Homman-Ludiyé, J. A. Bourne, The medial pulvinar: Function, origin and association with neurodevelopmental disorders. *J. Anat.* **235**, 507–520 (2019).
53. B. J. Casey *et al.*, The Adolescent Brain Cognitive Development (ABCD) study: Imaging acquisition across 21 sites. *Dev. Cogn. Neurosci.* **32**, 43–54 (2018).
54. D. C. Van Essen *et al.*, Data from "The Human Connectome Project: a data acquisition perspective". *Neuroimage* **62**, 2222–2231 (2012). Available at <https://www.humanconnectome.org/study/hcp-young-adult>. Accessed 1 May 2023.
55. K. Ugurbil *et al.*, Pushing spatial and temporal resolution for functional and diffusion MRI in the Human Connectome Project. *Neuroimage* **80**, 80–104 (2013).
56. M. F. Glasser *et al.*, The minimal preprocessing pipelines for the Human Connectome Project. *Neuroimage* **80**, 105–124 (2013).
57. J. L. Andersson, S. N. Sotiropoulos, Non-parametric representation and prediction of single- and multi-shell diffusion-weighted MRI data using Gaussian processes. *Neuroimage* **122**, 166–176 (2015).
58. J. L. R. Andersson, S. N. Sotiropoulos, An integrated approach to correction for off-resonance effects and subject movement in diffusion MR imaging. *Neuroimage* **125**, 1063–1078 (2016).
59. B. Patenaude, S. M. Smith, D. N. Kennedy, M. Jenkinson, A Bayesian model of shape and appearance for subcortical brain segmentation. *Neuroimage* **56**, 907–922 (2011).
60. B. Fischl, FreeSurfer. *Neuroimage* **62**, 774–781 (2012).
61. T. M. Achenbach, F. Verhulst, *Achenbach system of empirically based assessment (ASEBA)* University of Vermont, Research Center for Children, Youth, & Families, Burlington, VT, 2009.
62. D. J. Hagler Jr. *et al.*, Image processing and analysis methods for the adolescent brain cognitive development study. *Neuroimage* **202**, 116091 (2019).
63. A. M. Winkler, G. R. Ridgway, M. A. Webster, S. M. Smith, T. E. Nichols, Permutation inference for the general linear model. *Neuroimage* **92**, 381–397 (2014).
64. R. Watts, Code from "Sex and mental health are related to subcortical brain microstructure". GitHub. <https://github.com/ABCD-STUDY/RSI>. Deposited 3 July 2024.